Elastic electron scattering cross sections for molecular hydrogen

M. A. Khakoo* and S. Trajmar
Jet Propulsion Laboratory, California Institute of Technology, 4800 Oak Grove Drive, Pasadena, California 91109
(Received 19 April 1985; revised manuscript received 13 January 1986)

Using an electron-beam—molecular-beam apparatus and employing the relative flow technique, ratios of the differential elastic scattering cross sections (DCS's) of H_2 to He were measured at incident electron energies of 15—100 eV and angular range of 10°—125°. From these ratios, the absolute elastic DCS's for H_2 were determined by normalization to accurate, available elastic DCS's of He. Since pure rotational structure was not resolved in this work, the DCS's reported are the sum of elastic and rotational excitations of H_2 at room temperature. The reliability of the relative flow normalization to He was checked at each energy and angle by performing similar elastic DCS measurements on Ne (for which the cross sections are known). The resulting absolute Ne DCS's were found to be in good agreement (within 10%) with the Ne elastic DCS's measured previously [D. F. Register and S. Trajmar, Phys. Rev. A **29**, 1785 (1984)]. From the DCS's, integral and momentum-transfer cross sections were calculated. The present results are compared with other recent measurements.

I. INTRODUCTION

The elastic scattering of electrons from molecules plays an important part in energy transport in natural and man-made plasmas at subexcitation energies. Much effort has been made to determine the elastic differential cross sections (DCS's) for electron scattering from simple molecules, but there is still considerable disagreement among the presently available theoretical and experimental results even for the simplest molecular species, H_2. Recent reviews on this subject matter have been published by Trajmar *et al.*[1] and Csanak *et al.*[2] Very recently, Furst *et al.*[3] and Nishimura *et al.*[4] reported elastic differential and integral cross sections for H_2.

In our laboratory a systematic joint experimental and theoretical program was initiated to establish a consistent and accurate set of differential and integral elastic and inelastic electron-scattering cross sections for H_2 from near threshold to few hundred eV impact energies. As a necessary first step in this program, the elastic DCS's needed to be remeasured. The main reasons for this new measurement were (1) disagreement in available data, (2) recent improvements in relative flow techniques, (3) need for consistent elastic and inelastic data measured with the same apparatus under carefully controlled conditions.

In the present measurements, the relative flow technique[5,6] is applied with some further refinement. Helium was used as the standard gas and the relative flow method was applied both to H_2 and to Ne under the same experimental conditions. Since the elastic DCS's for Ne are well established,[7–10] this procedure minimized the systematic errors and served as a continuous check on the procedure.

II. EXPERIMENT

A. Apparatus

The electron spectrometer with minor modifications was the same as described earlier.[11] It was operated at a resolution of about 45 meV with an electron-beam current of approximately 3 nA. The angular divergence of the beam was approximately ±5° [full width at half maximum (FWHM)] at 15 eV incident electron energy and ±2° (FWHM) at 100 eV incident electron energy. The angular resolution of the scattered electron detector was ±3° (FWHM). Measurements were not carried out at impact energies lower than 15 eV since the collimation and the control of the electron beam was not satisfactory for quantitative work with this apparatus. The contact potential in the experiment remained consistently at −0.52 eV as observed by repeated measurements of the 19.3-eV resonance in He at 100° scattering angle. At the collision region, the electron beam was monitored by a Faraday cup made of molybdenum, sooted and mounted on a thin flexible titanium plate which enabled the Faraday cup to spring into place when the electron detector was rotated to angles greater than 25°. The Faraday cup did not contribute to any observable scattered electron signal at all the energies and scattering angles in this experiment. The zero scattering angle was determined in the conventional way by monitoring the inelastically scattered electrons having excited the 12.52-eV $X\,^1\Sigma_g^+$ $(v=0)\rightarrow C\,^1\Pi_u$ $(v=1)$ transition in H_2 or the 21.21-eV $^1S\rightarrow{}^1P$ transition in He as the detector was rotated through zero angle. It was possible to locate the approximate scattering angle to an accuracy of ±1°.

Although the collision region was at earth potential, it was additionally shielded by an earthed mesh of tantalum wire which had a slot for the detector nose cone and a gap for the electron gun nose cone, so that there were no stray electric fields from the rest of the surroundings of the collision region, e.g., charges on wire insulation, lens element voltages, etc. The magnetic field was reduced by a μ-metal shield to below 10 mG.

The gas beam was generated at right angles to the scattering plane by a 0.85-mm-diameter capillary array made up of ~100 capillaries of 3-mm length and 0.05 mm inside diameter. The array was fitted into the end of

a stainless steel tube of approximately 1.3 mm outside diameter. The tip of the array was placed at a distance of 3 mm from the electron-beam axis where it was found not to interfere with the electron beam and hence did not contribute to extra electron scattering.

B. Relative flow method

Details of this method were given by Srivastava *et al.*[5] with further refinements made by Trajmar and Register.[6] Using a crossed-beam arrangement, it is possible with this method to determine the elastic scattering DCS's of an unknown gas X by calibration to a gas A whose elastic DCS's are known. The elastic scattering intensities by the gas A, $N_e^A(E_0,\theta)$ (incident electron energy E_0, scattering angle θ), and by the gas X, $N_e^X(E_0,\theta)$, are measured under the same experimental conditions. (The electron-beam flux distribution, the detector efficiency, the target-gas-beam flux distribution and the overall geometry are the same for both gases A and X.) Under these conditions, the effective path length corrections for both gases will be identical to a good approximation. The angular dependences of the elastic DCS's are, in general, different for the two gases, and this introduces a small deviation in the effective path lengths, but the effect will be significant only when the angular dependence of the elastic DCS's for the two gases are very different and one of them changes abruptly with scattering angle. The stability of the electron beam while the gases were interchanged in the experiment was maintained by operating the gas-beam system such that the background pressure in the vacuum chamber remained low ($\leq 1\times10^{-6}$ Torr), and by monitoring the electron beam through the collision region throughout the experiment.

The central problem at present in the relative flow method is to ensure that the target-gas-beam flux angular distribution functions are identical for both gases. (Not the absolute flux but only the distributions are required to be the same.) This condition prevails if the molecular flow in the capillary tubes used to form the target beam is collisionless (the mean free path λ is larger than the length of the capillary tube). The gas densities associated with this flow regime ($P_G \leq 0.1$ Torr for H_2 in our case), however, are too low for adequate signal-to-noise requirements in scattering experiments. Fortunately, equal flux distributions for various gases can be maintained at higher flow rates (pressure) under certain conditions. The calculations of Olander and Kruger[12] show that for $K_L \gtrsim \gamma$ (where K_L is the Knudsen number, γ is the ratio of the tube diameter d to its length L) the angular distribution functions for any two gases will be the same provided that the head pressure behind the capillary is such that the mean free path λ of both gases is maintained equal [or in other words if the Knudsen number (λ/L) associated with the capillary tube at the high-pressure end of the tube is equal for both gases].[6] A similar conclusion can be drawn from the formalism of Giordmaine and Wang.[13] Under the above conditions, the scattering intensity ratio is to a good approximation

$$\frac{N_e^X(E_0,\theta)}{N_e^A(E_0,\theta)} = \frac{\sigma_X(E_0,\theta)\dot{n}_x\bar{V}_A}{\sigma_A(E_0,\theta)\dot{n}_A\bar{V}_X} = \frac{\sigma_X(E_0,\theta)}{\sigma_A(E_0,\theta)}\frac{\dot{n}_X}{\dot{n}_A}\sqrt{M_X/M_A}\,, \quad (1)$$

where $\bar{V}_A, \bar{V}_X$ are the average thermal velocities of the two gases and are replaced by the ratio of the inverse square roots of their molecular masses under the assumption that the two gases are at the same temperature. $\dot{n}_X$ and $\dot{n}_A$ are the flow rates for the two gases ($\sec^{-1}$) through the capillary source and σ_X and σ_A denote the corresponding cross sections. Brinkmann and Trajmar[14] have extended the same arguments to capillary arrays (assuming that no interaction occurs between beams from different capillary tubes). In our case $\gamma = 0.017$ and the condition $K_L \geq \gamma$ (or $\lambda \geq 2a$) restricts the head pressures to not greater than about 12 Torr in He and 8 Torr in H_2 and Ne.

Although the flux distributions are adjusted to be the same for the two gases [and cancel in Eq. (1)], we still have to determine the *ratio* of the flow rates. Since the head pressure behind the capillary is the most convenient parameter to monitor, it is necessary to calibrate the gas flow rate as a function of head pressure. Figure 1 shows the gas handling system used for this purpose. The procedure for this calibration was the following:

(i) The intermediate region (dotted in Figure 1) and the gas cylinder line for the gas of interest (in this example, gas X) was pumped down through V_R with V_L, V_G, and LV_A closed and V_R, LV_X, and RV_X open. The gas cylinder head valve V_X is closed. After roughing down to $\approx$10 mTorr, RV_X was closed, V_X opened and then RV_X gently opened to flush gas X through the system during which V_R was opened and closed several times to enable the gas to reach 1–2 lbs in^{-2} pressure in the intermediate region so that wall collisions of the gas X in this region could remove adsorbed impurities on the surfaces. LV_X was closed and after roughing down to $\approx$10 mTorr, V_R was closed and V_L,V_G opened to further evacuate the whole gas apparatus to pressures $\approx 10^{-4}$–10^{-5} Torr or lower, and the Baratron gauge base pressure reading was recorded.

(ii) The leak valve, LV_X was then opened to allow a sufficient flow of gas to take place through the apparatus and the Baratron gauge readings were recorded for steady flow when V_L closed and V_G opened and when V_L opened, V_G closed (respectively, P_G and P_L). It was observed that the ionization gauge reading (P_{IG}) was independent of the path the gas entered the vacuum tank, i.e., the pressure in the vacuum chamber or equivalently the flow rate of gas was dependent only on the magnitude of the pressure differential across the leak valve (LV_X) and that the pressure in the intermediate region "readjusted" to maintain the flow rate through LV_X equal to the gas flowing into the vacuum tank through the leak. This readjustment of intermediate region pressure leaves the pressure differential across LV_X practically unaffected. The pressure on the high-pressure side of LV_X is about 5 psi ($\approx$500 Torr) and the maximum change in pressure at the intermediate region was 3 Torr between P_G and P_L in this work which represents a 0.12% change in pressure differential across LV_X (see Table I).

(iii) With both V_G and V_L closed the pressure in the intermediate region P_B (read by Baratron) was allowed to

TABLE I. Representative samples of pressures versus flow rate measurements. Numbers in square brackets indicate exponents to base 10. For a description of parameters see text.

Gas	P_{IG} (Torr)	P_G (Torr)	P_L (Torr)	$\frac{dP}{dt}$ Torr sec^{-1}	$\dot{n}$ (sec^{-1})
H_2	5.6[−8]	3.17[−2]	8.0[−3]	1.15[−3]	5.74[14]
	1.5[−7]	3.13[−1]	4.75[−2]	1.46[−2]	7.28[15]
	8.4[−7]	1.64[0]	2.65[−1]	9.97[−2]	7.04[16]
	3.2[−6]	5.64[0]	7.87[−1]	4.37[−1]	3.08[17]
He	4.8[−8]	3.56[−2]	9.20[−3]	1.04[−3]	7.33[14]
	1.3[−7]	7.07[−1]	1.08[−1]	2.61[−2]	1.84[16]
	6.2[−7]	3.52[0]	5.68[−1]	1.70[−1]	1.20[17]
	1.2[−6]	6.91[0]	1.02[0]	3.80[0]	2.68[17]
Ne	1.3[−7]	8.81[−2]	1.71[−2]	1.30[−3]	9.16[14]
	5.7[−7]	2.11[0]	3.33[−1]	4.56[−2]	3.21[16]
	1.9[−6]	7.11[0]	9.62[−1]	1.85[−1]	1.30[17]
	3.1[−6]	10.73[0]	1.29[0]	2.90[−1]	2.04[17]

rise. By monitoring the rate-of-change of pressure with time (t) about the value P_G, we determine the quantity dP_B/dt. This procedure is repeated by opening V_L, letting the pressure P_B drop to below P_G and then repeating the whole procedure (iii). An average of at least ten such measurements of dP_B/dt were taken.

(iv) LV_X was then changed to a new leak flow rate setting and procedures (ii) and (iii) were repeated.

Although not necessary for the present work, the absolute flow rates can be easily determined for a given gas handling and capillary array system. Since the volume (dotted in Fig. 1) being filled in procedure (iii) is constant (V_0), one can relate the flow rate $\dot{n}$ (dn/dt) to the value dP_B/dt using the ideal gas law

$$PV_0 = nkT_0 \,, \tag{2}$$

where T_0 is the room temperature (=292 K), k is Boltzmann's constant, and n is the number of gas atoms (molecules). Differentiation and substitution of the numerical values of k and T_0, gives

$$V_0 \frac{dP}{dt} = 3.023 \times 10^{17} \frac{dn}{dt} \,, \tag{3}$$

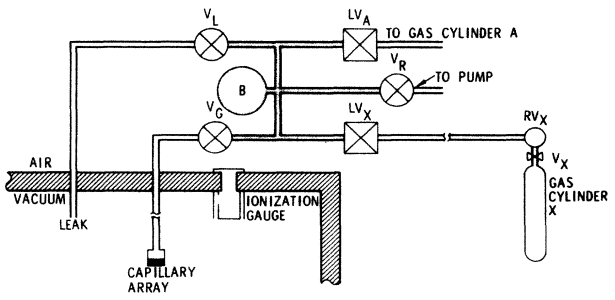

FIG. 1. Diagram of gas handling system used for the relative flow method. For description of symbols see text.

where dP/dt is in Torr sec^{-1}, V_0 in cm^3 and dn/dt in sec^{-1}.

V_0 was determined by disconnecting the roughing line at V_R (arrowed in Fig. 1) and inserting a known volume V_c at this point. Both V_0 and V_c were evacuated through V_L. Then V_L and V_R were closed and V_0 was filled with low-pressure gas through LV_x to P_1 (Torr). V_R was then opened and the new pressure P_2 (Torr) was measured. Boyle's Law gives V_0 in terms of P_1, P_2, and V_c

$$V_0 = \frac{P_2 V_c}{P_1 - P_2} \,. \tag{4}$$

In this experiment V_0 was found to be 21.3±2 cm^3 and hence the absolute form of Eq. (3) for this experiment was

$$\frac{dn}{dt} = 7.059 \times 10^{17} \frac{dP}{dt} \,. \tag{5}$$

Figure 2 shows typical flow rate times $\sqrt{M}$ values for various gases as a function of source head pressure. We found that the flow rates were linear and extrapolate to zero flow rate at zero pressure up to capillary backpressures of about 0.6 Torr. The very lowest part of this pressure region corresponds to free molecular flow (below about 0.05 Torr for He and even lower for Ne and H_2). In the major remainder part of this linear region the flow is not strictly molecular but is not significantly affected by collisions. At around 0.6 Torr there is a break in the curves and although the curve is not strictly linear above this pressure, it can be described to a very good approximation by a straight line up to about 5 Torr.

As we discussed in Sec. II B, the validity of Eq. (1) requires in our case that the capillary head pressure be not greater than about 12 Torr for He and 8 Torr for Ne and H_2. In order to achieve good signal-to-noise conditions and to remain in the flow regime where $K_L \geq \gamma$, it is desirable to carry out the scattering measurements at capillary back pressure in the 1 to 10 Torr region for He, Ne, and H_2. Table I gives typical pressure and flow-rate values obtained in this experiment.

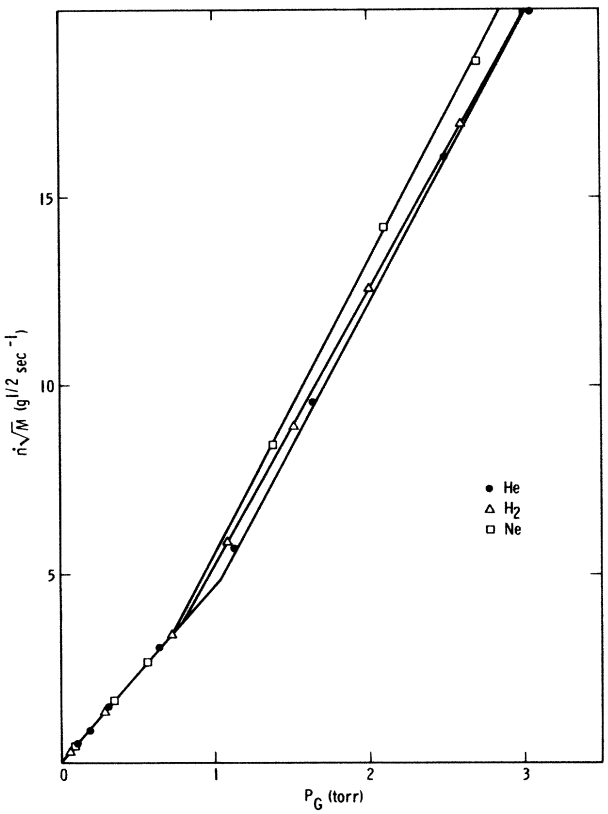

FIG. 2. Flow rate times $\sqrt{M}$ vs source pressure for H_2, He, and Ne.

C. Operating procedures

With the electron beam operating, and focused into the Faraday cup, H_2 is passed via LV_X through the capillary array at a source pressure (P_G) not exceeding 3 Torr and not around the region of the break in Fig. 2 (0.8 Torr). After the gas beam had stabilized, and the flow conditions were checked by observing the ionization gauge and Baratron gauge readings, measurements of scattered electron intensity were made at fixed impact energies and scattering angles by scanning the elastic peak and integrating the peak area. The data was stored and processed automatically in a multichannel analyzer which also subtracted the background obtained from the scattering outside of the elastic peak. This process was repeated at a fixed impact energy for a random sequence of angles through the angular range of 10° to 125° in 5° intervals. At least three measurements were made at each angle to ensure that stable conditions existed. The valve V_L was then opened and V_G was closed (Fig. 1) and this way the elastic contribution from the background gas was determined. This contribution was also subtracted from the measured elastic signal. At worst (at low impact energies), this background gave a 10% contribution to the scattered electron intensity. LV_X was closed, Fig. 1, and the H_2 was pumped out through V_L. V_L was closed and helium was passed through at high pressure (5 psi) into the dotted region (Fig. 1) and roughed out through V_R. This process was repeated several times. Then, LV_A and V_R were closed in sequence and V_G was opened. LV_A was opened to enable He to flow through the capillary and LV_A carefully adjusted to give the right pressure so that *the mean free path for He behind the capillary array was equal to that of H_2 during the H_2 elastic measurements.* In general this pressure could be achieved to a precision of 2%. The Baratron gauge reading was recorded and used to obtain the flow rate for He from Fig. 2. This flow rate together with the corresponding H_2 flow rate was then used in Eq. (1) to achieve the cross-section calibration. The elastic intensity measurements were repeated for He. Thereafter, a neon cylinder replaced the H_2 cylinder and after evacuation and flushing the gas feed lines, the elastic scattering intensity measurements were repeated for Ne again at a flow rate where the mean free path was equal to that of He (and H_2). In all cases the electron-beam current at the Faraday cup was found to be stable to 1%, otherwise the whole data set was rejected. These measurements yielded the elastic electron scattering intensities of H_2 and Ne relative to He as a function of angle at a fixed impact energy.

The above procedure was repeated at various impact energies until a minimum of three sets of data were obtained at each impact energy for each gas. From the intensity measurements the absolute elastic DCS's were obtained for H_2 and Ne by utilizing Eq. (1) and the elastic DCS's of He as given by Register *et al.*[15] The purpose of measuring Ne together with H_2 was to have an additional check on the calibration procedure since the Ne cross sections are fairly well established.

III. DISCUSSION OF RESULTS

A. Differential cross sections

Absolute DCS's for elastic electron scattering in H_2 were determined at impact energies of 15, 17.5, 20, 30, 40, 60, and 100 eV and for scattering angles of 10° to 125°. Table II gives a numerical tabulation of the DCS's and the data are plotted for comparison with recent measurements in Fig. 3. Error contributions from various sources and the overall errors are given in Table III. The flow rate error refers to the error associated with the flow rate versus pressure calibration.

In principle, from the calibration point of view, it would be most desirable to carry out the relative flow measurements under free molecular flow conditions in the capillary array. As previously stated, the target-gas densities corresponding to this flow region are very low resulting in weak scattering, large statistical error, and long time requirement. From a practical point of view we found that the optimum conditions for the measurements were obtained at P_G values corresponding to a few Torr where good statistics could be easily achieved but special attention has to be paid to operate with the proper flow conditions and maintaining the pressure in the experimental tank below the aforementioned limits. As a check on our procedures, we carried out relative flow calibrations at pressures ranging from 0.01 to 5 Torr on Ne and found that at $P_G \leq 0.1$ Torr the application of Eq. (1) yielded the

TABLE II. Summary of the present H_2 elastic electron scattering DCS's in $10^{-18}cm^2sr^{-1}$. Average error values are given for each impact energy.

Scattering Angle (deg)	Impact energy 15 eV	17.5 eV	20 eV	30 eV	40 eV	60 eV	100 eV
10						116	122
15				251	180	91.3	84.2
20	232	220	207	184	142	67.8	57.6
25	198	180	177	134	102	47.2	37.4
30	174	162	156	102	72.4	33.0	23.7
35	147	134	128	80.9	52.0	22.8	16.0
40	130	114	107	61.3	39.6	16.7	11.1
45	114	100	86.1	46.2	30.3	12.0	7.1
50	95.1	85.4	73.8	35.4	23.4	9.25	5.28
55	78.0	72.2	59.9	28.6	18.3	7.24	3.94
60	66.8	61.4	48.2	22.1	14.4	5.53	2.99
65	56.4	51.8	40.9	18.3	11.3	4.38	2.37
70	48.3	45.2	35.3	15.0	9.45	3.50	1.94
75	40.7	36.4	29.3	12.5	7.66	2.91	1.63
80	34.4	31.6	24.8	10.2	6.40	2.47	1.31
85	29.9	26.9	21.1	8.62	5.40	2.10	1.19
90	27.2	23.6	18.0	7.46	4.69	1.90	1.06
95	23.9	20.0	15.5	6.58	4.17	1.66	0.97
100	21.2	17.1	13.2	5.81	3.68	1.55	0.90
105	19.1	14.8	11.3	5.13	3.40	1.39	0.81
110	17.6	12.7	9.90	4.83	3.09	1.25	0.72
115	16.7	11.1	8.65	4.45	2.87	1.15	0.68
120	15.9	10.3	8.35	4.36	2.75	1.08	0.66
125	15.4	9.41	8.11	4.18	2.67	1.02	0.64
Error	13%	13%	12%	13%	13%	14%	16%

proper DCS values at any pressures selected for He and Ne. While at higher source pressures we were able to obtain the correct DCS values for Ne from Eq. (1) only if the flow rates (or pressures) for He and Ne were selected to correspond to equal mean free paths behind the capillary array.

The DCS calibrations for H_2 against He were carried out with both gases under the proper (equal mean free path) conditions. The lowest angle at which reliable measurements could be carried out depended on the impact energy (electron-beam divergence).

At lower impact energies, i.e., 15—40 eV, our measurements (see Fig. 3) are in better overall agreement with the measurements of Shyn and Sharp[16] than with the earlier data of Srivastava *et al.*[5] (renormalized to more recent He DCS's by Trajmar *et al.*[1]). The experimental procedure used by Srivastava *et al.* was very similar to the present one, i.e., a crossed-beam geometry and relative flow calibration. However they determined the flow rate by using both mass and volume flow meters. The capillary back

TABLE III. Summary of errors for the differential cross sections. Total error is the square root of the sum of the squares of the individual errors.

Impact Energy (eV)	Source of error (%) Normalization Error (relative flow)	Helium DCS Data Precision	Statistical Error (average)	Electron Beam Stability	Gas Beam Stability	Angular Setting Precision	Flow Rate Error (average)	Total Error (%)
15.0	8.1	5	2.7	1	0.5	2	8	12.9
17.5	7.3	7.1	2.5	1	0.5	2	8	13.4
20.0	6.9	5	1.8	1	0.5	1.5	8	12.0
30.0	7.0	7	2.2	1	0.5	1.5	8	13.1
40.0	8.7	5.5	2.5	1	0.5	1.2	8	13.4
60.0	10.0	6	2.4	1	0.5	1.0	8	14.4
100.0	11.0	7.5	3.0	1	0.5	1.0	8	15.9

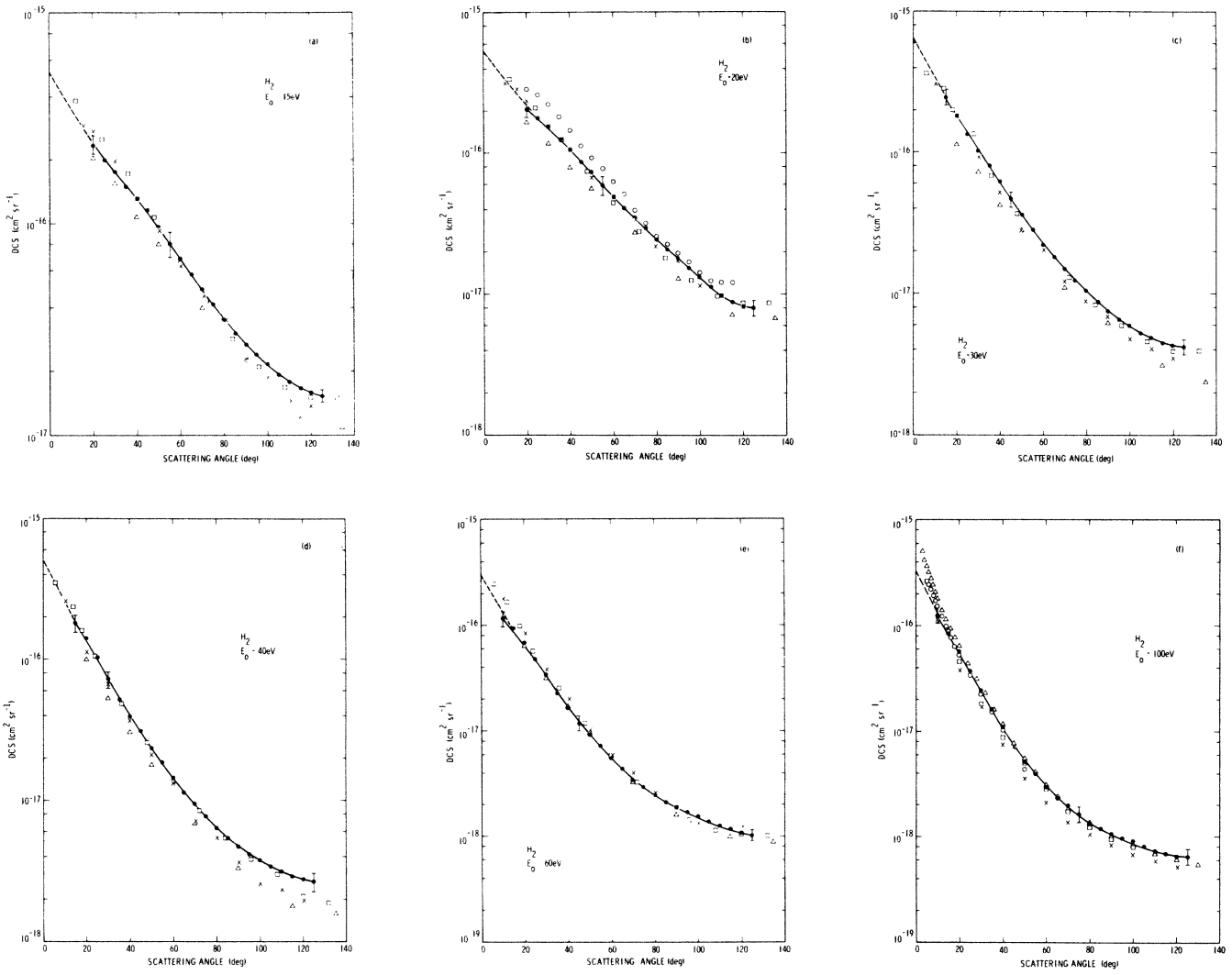

FIG. 3. Comparison of present DCS with other recent experimental works. (a) $E_0=15$ eV. ⧓ (joined by solid line), present work; □, Shyn and Sharp (Ref. 16); △, Srivastava *et al.* (Ref. 5) as renormalized by Trajmar *et al.* (Ref. 1); ×, Nishimura *et al.* (Ref. 4). The dashed line represents extrapolation to zero angle. (b) $E_0=20$ eV, same as for (a) and ○, Furst *et al.* (Ref. 3). (c) $E_0=30$ eV, same as for (a). (d) $E_0=40$ eV, same as for (a). (e) $E_0=60$ eV, same as for (a). (f) $E_0=100$ ev, ⧓ (joined by solid line), present work; △, Fink *et al.* (Ref. 17); ○, van Wingerden *et al.* (Ref. 18).

pressure in their experiments was about 1 Torr both for He and for H_2. This could, in principle, influence the relative target-density distribution but in practice the effect is negligible at this source pressure compared to other errors. The somewhat larger uncertainty in their measurements is due to the larger statistical spread in the scattering signal (lower target density) and larger uncertainties and systematic errors associated with the use of flow meters at low pressures. The results of Shyn and Sharp were also obtained from crossed-beam experiments using relative flow calibration but only for effective path-length correction. The absolute normalization of their data was made by filling up their whole chamber with He to a given pressure and measuring the scattering intensity and then repeating the same with H_2 gas. In this method one does not have to rely on canceling geometrical factor in Eq. (1) by equalizing mean free paths. The method is, however, susceptible to errors due to the fact that the electron beam may well be differently affected by different gases. Shyn and Sharp normalized their relative cross sections at one impact energy (10 eV) to He and, since their electron detector contained no electron lenses, they needed no correction related to the dependence of the detector efficiency as a function of electron energy. The DCS's obtained by Nishimura *et al.*[4] using very similar techniques to ours are in agreement with the present results within the combined error limits. Our 20-eV DCS's are also compared with the recent 19-eV work of Furst *et al.*,[3] who used relative flow techniques under free molecular flow conditions and a time-of-flight technique to discriminate between elastically and inelastically scattered electrons. As can be seen, their data are in reasonably good agreement with the present results in the 70°—105° range, but at smaller scattering angles and above 105° the two

TABLE IV. Summary of integral and momentum transfer cross sections (10^{-18} cm^2 units).

	Integral				Momentum Transfer		
E_0 (eV)	Ref. 5[a]	Ref. 16	Ref. 4	Present[b]	Ref. 16	Ref. 4	Present[b]
15	589	755	717	704 (16)	329	320	326 (14)
17.5				627 (16)			273 (14)
20	415	561	574	555 (16)	211	227	221 (13)
30	230	336	325	363 (16)	102	97.8	108 (14)
40	170	250	223	252 (16)	64	58.5	69.5 (14)
60	100	127	135	115 (17)	29	32.2	27.3 (15)
100		77	64.8	83.4 (19)	15	12.7	17.4 (17)

[a]As renormalized by Trajmar *et al.* (Ref. 1) based on more recent He elastic cross sections.
[b]Numbers in parentheses refer to the percentage error.

sets of data differ somewhat. The 1 eV impact energy difference is not likely to be the reason for this disagreement since our 17.5-eV data are very similar to our 20-eV data indicating that the shape and magnitude of the elastic He DCS's is not changing drastically over this impact energy range.

At the impact energy of 60 eV all four experimental DCS's are in excellent agreement except at 10° where the present cross section is smaller by about 50%. At low scattering angles, due to the strong forward scattering, the angular acceptance profile of the detector begins to influence the data and the geometrical effects become more critical. These effects may account for the difference.

At 100 eV excellent agreement with the previous measurements of Fink *et al.*[17] and van Wingerden *et al.*[18] is found except for the deviations at small scattering angles.

There have been a fairly large number of theoretical calculations carried out for predicing the elastic DCS's for H_2. In general, many of them show good agreement with experimental data when polarization and exchange effects are properly accounted for. For more detailed discussion of this matter see Refs. 2, 19, and 20.

B. Integral cross sections

To integrate the cross sections, we fitted the absolute H_2 DCS's to a partial-wave effective range (see, e.g., Ref. 15) expansion of the form

$$\sigma_A(\theta)=|f(\theta)|^2 , \tag{6a}$$

$$f(\theta)=\frac{1}{2ik}\sum_{l=0}^{L}\{(2l+1)[\exp(2i\delta_l)-1]P_l(\cos\theta)\} + C_L(\theta) , \tag{6b}$$

$$C_L(\theta)=\pi\alpha k\left[\tfrac{1}{3}-\tfrac{1}{2}\sin(\tfrac{1}{2}\theta)-\sum_{l=1}^{L}\frac{P_l(\cos\theta)}{(2l+3)(2l-1)}\right] , \tag{6c}$$

where δ_l is the lth partial-wave phase shift, and α is the dipole polarizability of H_2 ($=5.18a_0^2$, from Ref. 20), θ is the scattering angle and k is the electron momentum in atomic units. This was found to be preferable to any arbitrary polynomial since it is expected to have some physical significance. Fits were made with L values up to 5. This fit was then used to extrapolate the DCS's to 0° and to 180° and integration yielded the elastic integral and momentum-transfer cross sections tabulated in Table IV. The errors associated with the extrapolation and integration of the DCS's are judged to be about 10% for integral and 5% for momentum-transfer cross sections. These errors are combined with the DCS errors and are also given in Table IV. The integral elastic cross section of Shyn and Sharp and Srivastava *et al.* are also given for comparison.

ACKNOWLEDGMENTS

The authors would like to thank J. C. Nickel, J. W. McConkey, and D. F. Register for valuable discussions during the course of this work. The research described in this paper was performed at the Jet Propulsion Laboratory, California Institute of Technology, and sponsored by the National Aeronautics and Space Administration, by the National Science Foundation, and by NATO Scientific Affairs Division. One of the authors (M.A.K.) would like to thank the National Research Council for a grant during part of this work.

*Present address: Physics Department, University of Windsor, 401 Sunset Avenue, Windsor, Ontario, Canada N9B 3P4.

[1]S. Trajmar, D. F. Register, and A. Chutjian, Phys. Rep. **97**, 239 (1983).
[2]G. Csanak, D. C. Cartwright, S. K. Srivastava, and S. Trajmar, in *Electron-Molecule Interactions and Their Applications,* edited by L. G. Christophorou (Academic, New York, 1984), Chap. I.
[3]J. Furst, M. Mahgerefteh, and D. E. Golden, Phys. Rev. A **30**, 2256 (1984).
[4]H. Nishimura, A. Danjo, and H. Sugahara, J. Phys. Soc. Jpn. **54**, 1757 (1985).
[5]S. K. Srivastava, A. Chutjian, and S. Trajmar, J. Chem. Phys. **63**, 2659 (1975).
[6]S. Trajmar and D. F. Register, in *Electron-Molecule Collisions,* edited by I. Shimamura and K. Takayanagi (Plenum, New York, 1984).
[7]J. F. Williams and H. Crowe, J. Phys. B **8**, 2233 (1975).

[19]N. F. Lane, Rev. Mod. Phys. **52**, 29 (1980).
[20]T. L. Gibson, M. A. P. Lima, K. Takatsuka, and V. McKoy, Phys. Rev. A **30**, 3005 (1984).
[8]D. F. C. Brewer, W. R. Newell, S. F. W. Harper, and A. C. H. Smith, J. Phys. B **14**, L749 (1981).
[9]D. Andrick (private communication).
[10]D. F. Register and S. Trajmar, Phys. Rev. A **29**, 1785 (1984).
[11]A. Chutjian, J. Chem. Phys. **61**, 4279 (1974).
[12]D. R. Olander and V. Kruger, J. Appl. Phys. **41**, 2769 (1970).
[13]J. A. Giordmaine and T. C. Wang, J. Appl. Phys. **31**, 463 (1960).
[14]R. T. Brinkmann and S. Trajmar, J. Phys. E **14**, 245 (1981).
[15]D. F. Register, S. Trajmar, and S. K. Srivastava, Phys. Rev. A **21**, 1134 (1980).
[16]T. W. Shyn and W. E. Sharp, Phys. Rev. A **24**, 1734 (1981).
[17]M. Fink, K. Jost and D. Hermann, Phys. Rev. A **12**, 1374 (1975).
[18]B. van Wingerden, E. Weigold, F. J. de Heer, and K. J. Nygard, J. Phys. B **10**, 1345 (1977).

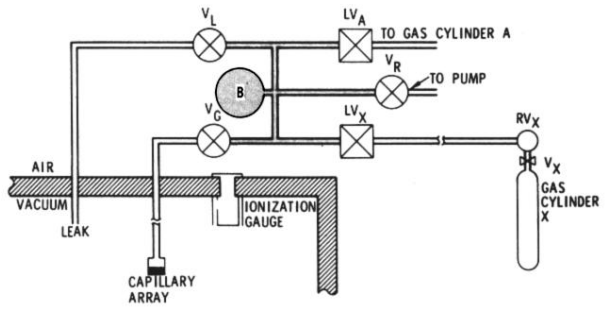

FIG. 1. Diagram of gas handling system used for the relative flow method. For description of symbols see text.